Inorganic Chemistry

Article

pubs.acs.org/IC

Hemilabile and Bimetallic Coordination in Rh and Ir Complexes of NCN Pincer Ligands

Giulia Mancano,[†] Michael J. Page,[†] Mohan Bhadbhade,[†,‡] and Barbara A. Messerle*[,†]

[†]School of Chemistry and [‡]Mark Wainwright Analytical Centre, The University of New South Wales, Kensington, Sydney, NSW 2052, Australia

Supporting Information

ABSTRACT: Two new pincer ligands have been developed that contain a central N-heterocyclic carbene (NHC) moiety linked to two pendant pyrazole groups by either a methylene (NCN^{me}) or ethylene (NCN^{et}) chain. The coordination of these two ligands to rhodium and iridium resulted in a variety of binding modes. Tridentate coordination of the ligands was observed in the complexes $[Rh(NCN^{me})(COD)]BPh_4$ (**8**), $[Ir(NCN^{me})(COD)]BPh_4$ (**10**), $[Rh(NCN^{et})(CO)_2]BPh_4$ (**13**), and $[Ir(NCN^{me})(CO)_2]BPh_4$ (**14**), and monodentate NHC coordination was observed for $[Ir(NCN^{me})_2(COD)]$-BPh_4 (**11**) and $[Ir(NCN^{et})_2(COD)]BPh_4$ (**12**). Both tridentate and bidentate coordination modes were characterized for $[Rh(NCN^{et})(COD)]BPh_4$ (**9**) in the solution and solid state, respectively, while an unusual bridging mode was observed for the bimetallic complex $[Rh(\mu\text{-}NCN^{me})(CO)]_2(BPh_4)_2$ (**15**). The impact of this diverse coordination chemistry on the efficiency of the complexes as catalysts for the addition of NH, OH, and SiH bonds to alkynes was explored.

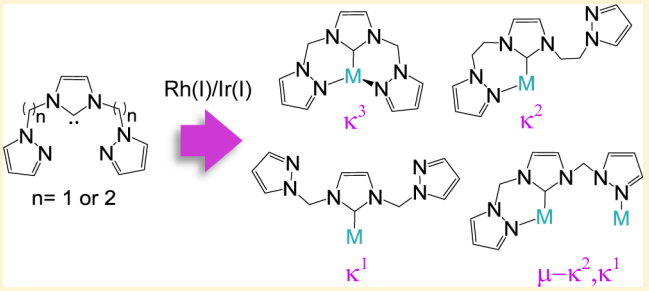

INTRODUCTION

The addition of heteroatom−hydrogen bonds to unsaturated carbon−carbon bonds is a selective and atom efficient route toward the formation of a wide range of new C−X bonds (X = B, N, O, Si, P, S).[1] The intramolecular cyclization of unsaturated carbon−carbon bonds tethered to NH or OH groups also provides access to a range of heterocyclic structures that are of biological significance (e.g., pyrroles, indoles, spiroketals, lactones).[1d] Therefore, the development of catalysts that facilitate such reactions in a selective and efficient manner is of great importance. Lanthanide, alkaline earth, and both early and late transition metal complexes have been used to catalyze the addition of X−H bonds to alkynes and alkenes, and of these, the low oxophilicity and high functional group tolerance of late transition metal complexes make them especially versatile catalysts for this process.[1,2]

The development of pincer ligands to support highly active transition metal catalysts has proven to be a particularly productive field of research in recent decades.[3] The typically rigid meridional coordination of a pincer ligand often affords complexes of high stability, increasing the lifetime of the catalyst and its tolerance for harsh reaction conditions. Several reports have highlighted the use of pincer ligand containing complexes of Ti, Zr, Hf, Ni, Pd, Pt, Rh, and Ir (Figure 1) as catalysts for the addition of OH, NH, or SiH bonds to alkynes.[4−6] The Ni PCP pincer complex **1** was recently reported to catalyze the hydroamination and hydroalkoxylation of acrylonitrile.[5e] Both Zr and Hf complexes of **2a** and **2b** were shown to catalyze the cyclization of primary and secondary aminoalkenes.[4d] The Rh and Ir CCC pincer complexes of **3a** and **3b** were also efficient catalysts for the cyclization of aminoalkenes,[6c] while the analogous Rh complex **4** catalyzed the hydrosilylation of alkynes.[6b] The Ir PNC pincer complex **5** was a potent catalyst for the intra- and intermolecular hydroamination of alkynes.[6a]

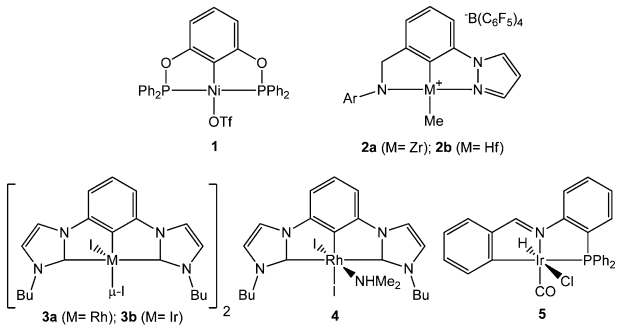

Figure 1. Pincer complexes used for the catalyzed addition of X−H bonds to alkynes and alkenes.

It has been observed in many metal catalyzed processes that a dynamic hemilabile coordination of a multitopic ligand can lead to significantly enhanced reaction rates.[7] The temporary dissociation of a secondary coordinating group can allow the complex to adapt to the steric and electronic requirements of the reaction while maintaining the stability afforded by a

Received: May 18, 2014
Published: September 24, 2014

formally chelated ligand coordination. Such hemilabile coordination has frequently been reported for metal complexes containing a pincer ligand where the temporary dissociation of a side arm donor group is necessary for a reaction to proceed.[8] Milstein and co-workers have shown that hemilabile pincer ligand coordination plays an important role in CH and CC bond cleavage reactions at Rh(III),[9] as well as in the Ru(II) catalyzed coupling of alcohols and amines to form amides.[10]

The design of pincer ligands that exhibit controlled and tunable hemilabile behavior remains a significant challenge.[11] Pincer ligands that contain a strongly coordinating N-heterocyclic carbene (NHC) as the central donor group and weakly coordinating side arms are ideally suited for enabling hemilabile coordination (Figure 2). The robust NHC−metal

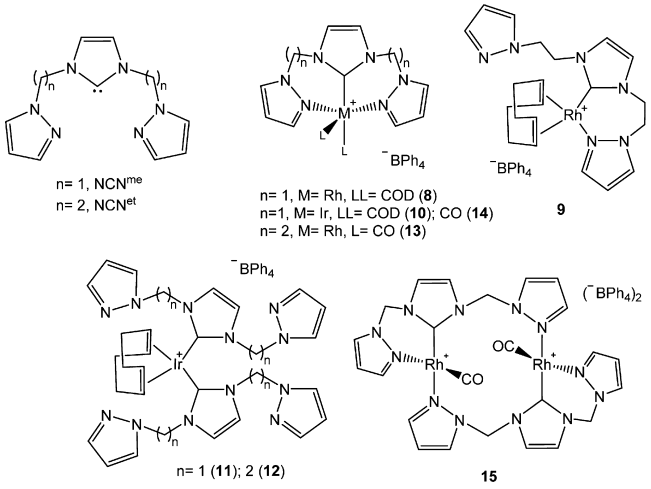

Figure 2. New NCN^{me} (**6**) and NCN^{et} (**7**) ligands and their complexes with Rh(I) and Ir(I).

bond can firmly anchor the ligand to the metal center, and at the same time the strongly electron donating nature of the carbene can help stabilize an unsaturated metal center.[12] The NHC ring can also be substituted at the N-positions with a wide range of side arm donor groups.[13] Currently, few pincer ligands containing a central NHC donor with weakly coordinating side arms have been reported and the catalytic properties of their complexes remain largely unexplored.[14]

Here we report the synthesis of two new pincer ligands (NCN^{me} and NCN^{et}, Figure 2) that contain a central NHC donor linked to two pyrazole groups by either a methylene or ethylene chain. The coordination of these ligands to Rh(I) and Ir(I) led to a surprisingly diverse number of coordination modes (Figure 2), suggesting the ligands are likely to exhibit hemilabile coordination. The impact of hemilabile pincer coordination on the efficiency of these Rh and Ir complexes as catalysts for the addition of NH, OH, and SiH bonds to alkynes is also described.

RESULTS AND DISCUSSION

Synthesis of Ligand Precursors 6 and 7. The imidazolium ligand precursors $NCN^{me}.HBPh_4$ (**6**) and $NCN^{et}.HBPh_4$ (**7**) were synthesized by the reaction of either chloromethylpyrazole or 2-bromoethylpyrazole (respectively) with half an equivalent of trimethylsilyl imidazole in refluxing toluene (Scheme 1). After 16 h a viscous brown oil had formed and upon exchange of the halide anion with $NaBPh_4$ the desired products were isolated as crystalline white solids (yield

Scheme 1

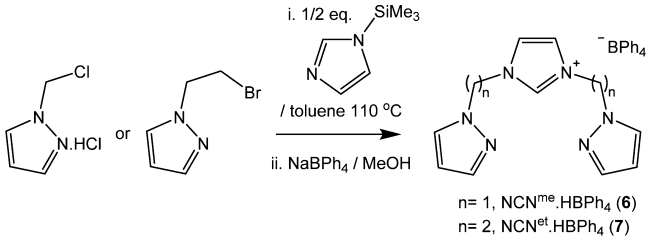

= 42% (**6**); 72% (**7**)). The ^1H NMR spectra (400 MHz, dmso-d_6) of **6** and **7** contain a characteristic high frequency singlet resonance for the imidazolium NC*H*N proton at 9.62 and 8.72 ppm, respectively.

Synthesis of Rh(I) 1,5-Cyclooctadiene Complexes $[Rh(NCN^{me})(COD)]BPh_4$ (8) and $[Rh(NCN^{et})(COD)]BPh_4$ (9). The coordination of the imidazolium ligand precursor $NCN^{me}.HBPh_4$ (**6**) to rhodium(I) was achieved by reaction of **6** with sodium ethoxide and $[Rh(\mu\text{-Cl})(COD)]_2$ in THF at room temperature (Scheme 2). After several hours the volatiles were removed and the residue was stirred in dichloromethane for 30 min to facilitate the elimination of NaCl from the mixture. The desired product $[Rh(NCN^{me})(COD)]BPh_4$ (**8**) was then isolated from solution by the addition of pentane. The characterization of **8** by ^1H and ^{13}C NMR spectroscopies indicated a tridentate coordination of the NCN^{me} ligand with both pyrazole groups occupying equivalent environments. The X-ray structure of **8** (Figure 3) revealed the NCN^{me} ligand to be bound in a facial manner to the metal center, as opposed to the expected meridional coordination typical of a pincer ligand framework. Complex **8** assumes a distorted trigonal bipyramidal geometry where the primary axis is occupied by the carbene and one COD alkene donor, with the second COD alkene and the two pyrazole donors forming the equatorial plane. The axial plane of symmetry that bisects the position of the two pyrazole groups in the solid state is consistent with the observation of only one set of pyrazole resonances in the ^1H NMR spectrum, suggesting the solution and solid state structures are equivalent.

Reaction of the ligand precursor $NCN^{et}.HBPh_4$ (**7**), which contains an ethylene bridge between the NHC and pyrazole donor groups, with sodium ethoxide and $[Rh(\mu\text{-Cl})(COD)]_2$ in methanol led to the formation of $[Rh(NCN^{et})(COD)]BPh_4$ (**9**) as the sole product. Characterization of **9** in solution indicated a symmetrical tridentate coordination of the NCN^{et} ligand with both pyrazole groups occupying equivalent environments. Intriguingly, the X-ray crystal structure of **9** (Figure 3) showed that in the solid state the NCN^{et} ligand is coordinated in an unsymmetrical bidentate fashion where the NHC donor and only one pyrazole donor are coordinated to Rh, giving a square planar geometry. To investigate the possibility that the symmetrical solution structure of **9** was actually the result of a bidentate coordination of the NCN^{et} ligand undergoing rapid exchange between bound and unbound pyrazole groups, the complex was analyzed at low temperature. No significant change in the ^1H NMR spectrum of **9** was observed at any temperature down to 190 K, indicating that any such exchange processes are unlikely and that a tridentate ligand coordination does indeed persist in solution. The fact that both tridentate and bidentate coordination modes were observed for the NCN^{et} ligand of **9** would suggest a relatively small difference in energy between these two configurations and a high likelihood of hemilabile behavior.

dx.doi.org/10.1021/ic501158x | *Inorg. Chem.* 2014, 53, 10159−10170

Scheme 2

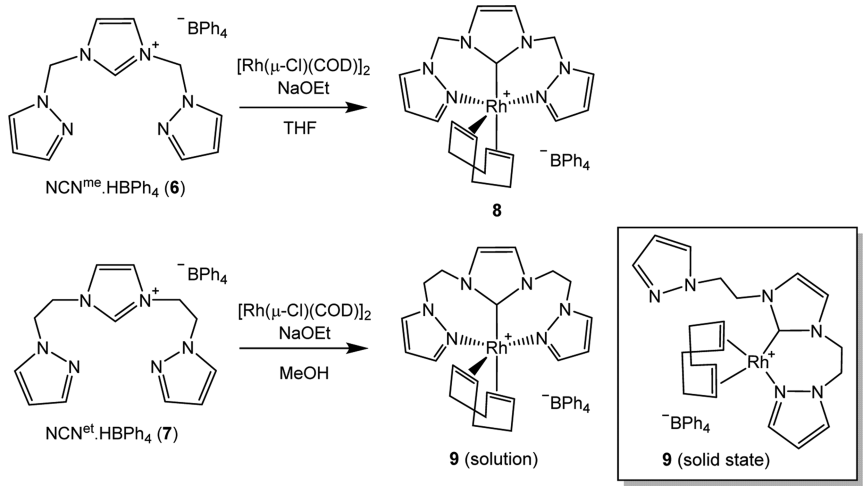

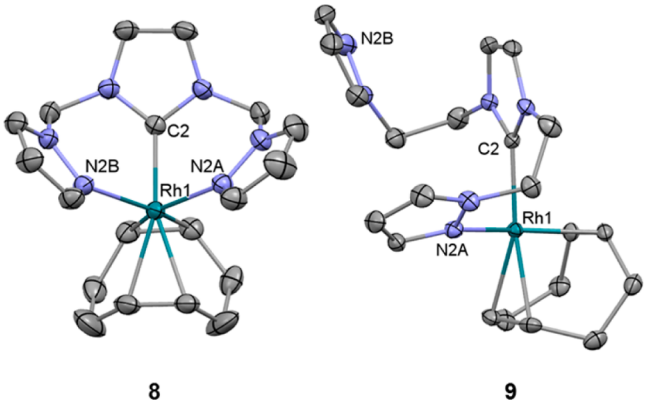

Figure 3. X-ray structures displaying the cationic fragments of $[Rh(NCN^{me})(COD)]BPh_4$ (**8**) and $[Rh(NCN^{et})(COD)]BPh_4$ (**9**) with ellipsoids shown at 30% probability.

Synthesis of Ir(I) 1,5-Cyclooctadiene Complexes $[Ir(NCN^{me})(COD)]BPh_4$ (10), $[Ir(NCN^{me})_2(COD)]BPh_4$ (11), and $[Ir(NCN^{et})_2(COD)]BPh_4$ (12). Reaction of the methylene bridged ligand precursor $NCN^{me}.HBPh_4$ (**6**) with sodium ethoxide and $[Ir(\mu\text{-}Cl)(COD)]_2$ in methanol afforded two distinct complexes (Scheme 3). The major product of the reaction $[Ir(NCN^{me})(COD)]BPh_4$ (**10**, yield = 46%) contained the NCN^{me} ligand coordinated in a tridentate fashion, whereas the minor product $[Ir(NCN^{me})_2(COD)]BPh_4$ (**11**, yield = 12%) contained two NCN^{me} ligands, each coordinated to iridium in a monodentate fashion through the NHC donors only. Reaction of the ethylene bridged ligand precursor $NCN^{et}.HBPh_4$ (**7**) with sodium ethoxide and $[Ir(\mu\text{-}Cl)(COD)]_2$ in methanol afforded only the analogous bis-carbene complex $[Ir(NCN^{et})_2(COD)]BPh_4$ (**12**) in modest yield (16%). The longer ethylene bridge between the NHC and pyrazole donors appears to prevent a tridentate coordination of the NCN^{et} ligand to iridium.

Complexes **10** and **11** were characterized by X-ray crystallography (Figure 4). (The X-ray structure of complex **12** was also obtained and is reported in the Supporting Information). The structure of complex **10** is similar to that obtained for the corresponding Rh(I) complex **8** with the NCN^{me} ligand coordinated in a facial manner to yield a trigonal

Scheme 3

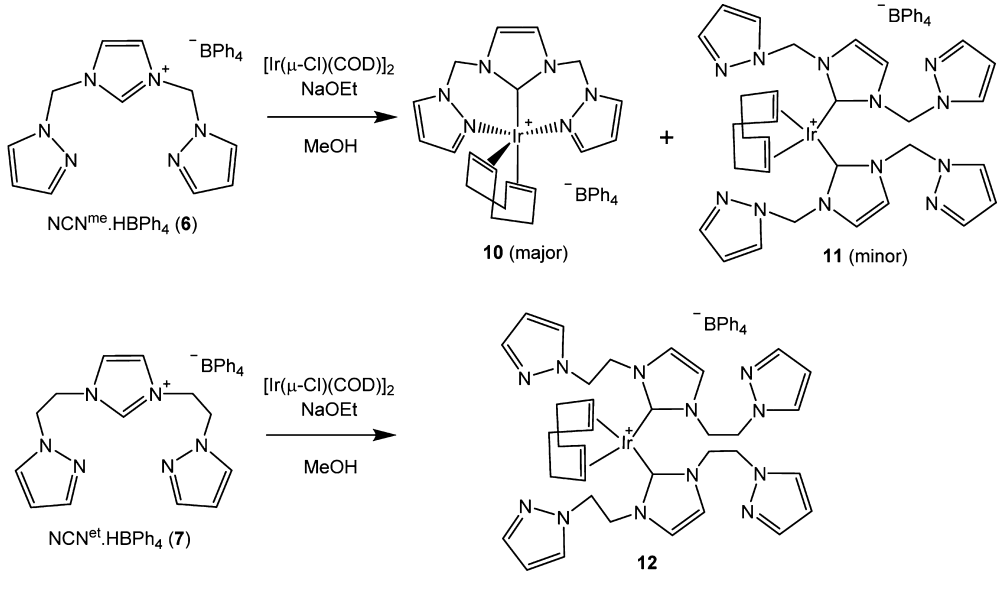

dx.doi.org/10.1021/ic501158x | Inorg. Chem. 2014, 53, 10159−10170

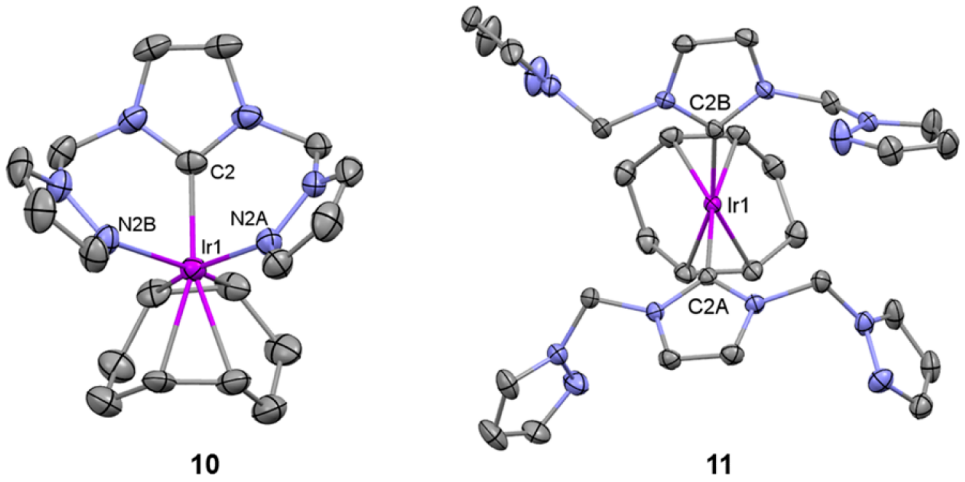

Figure 4. X-ray structures displaying the cationic fragments of [Ir(NCN^{me})(COD)]BPh$_4$ (**10**) and [Ir(NCN^{me})$_2$(COD)]BPh$_4$ (**11**) with ellipsoids shown at 30% probability.

Scheme 4

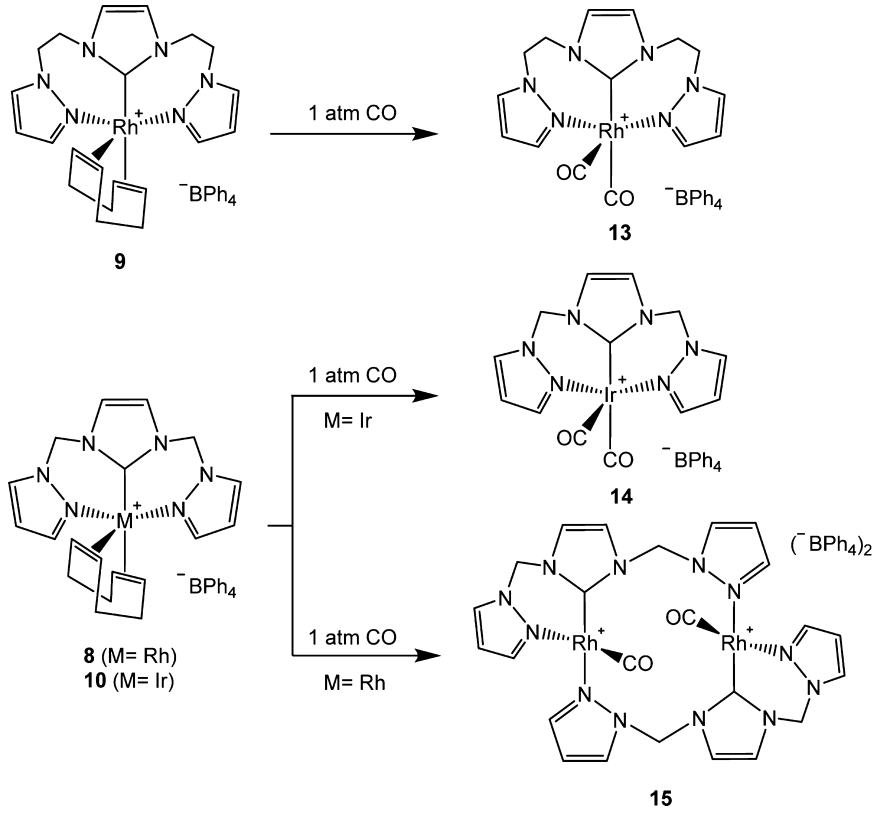

bipyramidal complex geometry. The structure of **11** clearly displays two NCN^{me} ligands coordinated solely through the NHC donor groups yielding a square planar complex geometry. The monodentate coordination of the ligands also results in a lengthening of the Ir−NHC bond distances for **11** (2.047(3) and 2.046(3) Å) relative to the Ir−NHC bond distance in **10** (1.996(4) Å), where all three donor groups are coordinated.

Synthesis of Rh(I) and Ir(I) CO Complexes [Rh(NCN^{et})(CO)$_2$]BPh$_4$ (13), [Ir(NCN^{me})(CO)$_2$]BPh$_4$ (14), and [Rh(NCN^{me})(CO)]$_2$(BPh$_4$)$_2$ (15). Displacement of the COD ligand from complexes **8**, **9**, and **10** with CO was achieved by exposing a solution of the complex to 1 atm of carbon monoxide (Scheme 4). For complexes **9** and **10** the reaction was performed in acetone-d_6 and the reaction progress was monitored in situ using ^{1}H NMR spectroscopy. Displacement of the COD ligand from **9** and **10** proceeded cleanly within minutes to afford the dicarbonyl complexes [Rh(NCN^{et})(CO)$_2$]BPh$_4$ (**13**) and [Ir(NCN^{me})(CO)$_2$]BPh$_4$ (**14**), respectively. The ^{1}H and ^{13}C NMR spectra indicate the tridentate coordination of the pincer ligands is retained in each case, while Fourier transform infrared (FTIR) spectra of the solutions revealed two CO stretching bands (**13** = 2091, 2034 cm^{-1}; **14** = 2081, 2013 cm^{-1}) consistent with the presence of two CO ligands on each metal. Unfortunately, when the solutions were degassed to remove CO, the complexes **13** and **14** were observed to degrade over several hours, leading to a multitude

dx.doi.org/10.1021/ic501158x | *Inorg. Chem.* 2014, 53, 10159−10170

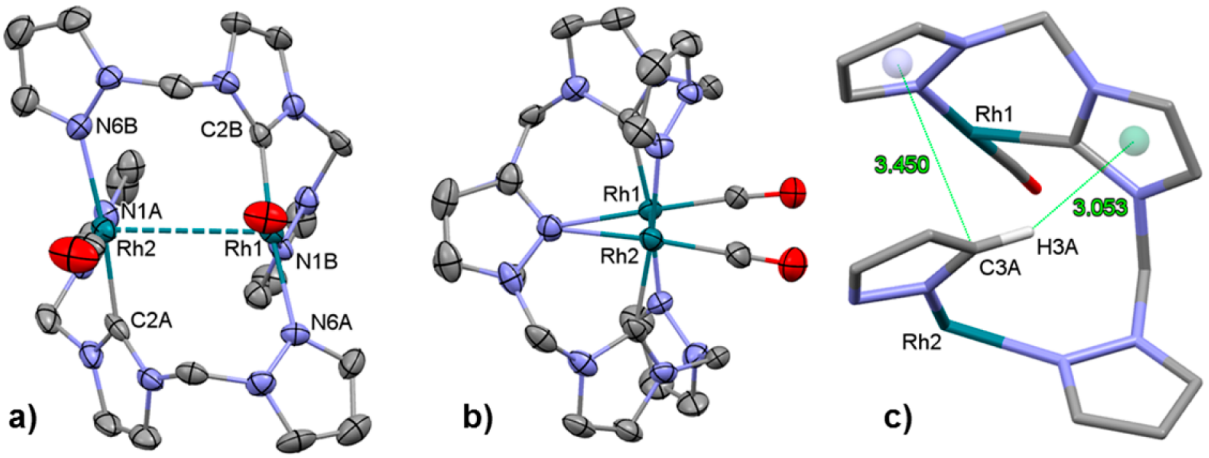

Figure 5. X-ray structure displaying the cationic fragment of $[Rh(NCN^{me})(CO)]_2(BPh_4)_2$ (**15**) viewed along (a) the Rh−CO axis and (b) the Rh−Rh axis (ellipsoids shown at 30% probability, Rh1−Rh2 = 3.3413(7) Å). (c) Short contacts observed within the structure of **15**.

of decomposition products. The instability of **13** and **14** in the absence of a CO atmosphere therefore precluded the isolation of these complexes. Rh(I) and Ir(I) complexes that contain a tridentate ligand group can form highly reactive complexes upon coordination of CO, where an increased disposition toward the formation of reactive metal hydrides has been noted previously.[15] An excess of CO may inhibit such reactivity in the case of complexes **13** and **14** through kinetic competition for vacant coordination sites on the metal. This stabilizing influence would disappear upon removal of the CO atmosphere, thereby initiating complex decomposition.

Reaction of $[Rh(NCN^{me})(COD)]BPh_4$ (**8**) with carbon monoxide did not result in the expected monomeric dicarbonyl complex but instead led to formation of the bimetallic complex $[Rh(\mu\text{-}NCN^{me})(CO)]_2(BPh_4)_2$ (**15**) (Scheme 4). The NCN^{me} ligand in **15** coordinates in an unusual bridging mode binding through the NHC and one pyrazole donor to one Rh center while the second pyrazole donor coordinates to the other Rh center. Both NCN^{me} ligands occupy equivalent environments, leading to a single set of ligand resonances in the ^1H and ^{13}C NMR spectra of **15**. Each Rh center coordinates to only one CO ligand, in contrast to the dicarbonyl complexes **13** and **14**, with both CO ligands occupying equivalent environments as evidenced by a single ^{13}CO resonance at 190.5 ppm (d, $^1J_{Rh-C}$ = 78 Hz) in the ^{13}C NMR spectrum (150 MHz, acetone-d_6, 193 K). The FTIR spectrum of **15**, which was acquired in both the solid state (KBr) and in solution (dimethyl sulfoxide (dmso)), revealed a single CO stretching frequency at 1998 cm^{-1}, confirming the presence of a single CO ligand at each Rh.

The solid state structure of **15** (Figure 5) shows that the two Rh centers are bound in a square planar geometry. The complex planes are aligned in a parallel fashion with an intermetallic Rh−Rh distance of 3.3413(7) Å. This distance is consistent with a weak metal−metal interaction between the two Rh centers.[16] The NHC and CO ligands are *trans* to the weaker pyrazole donors. Both CO ligands point in the same direction, giving the complex an approximate C_2 rotational symmetry along the N−Rh−CO axis. Slight distortion to the solid state structure, however, results in different metrics for each half-unit of the dimer. Interestingly, the proton at the 3-position of the pyrazole ring that is located *trans* to CO (i.e., H3A in Figure 5c) is positioned directly above the NHC ring of the second ligand ($H3A-NHC_{centroid}$ = 3.053 Å). This would account for the strong shielding observed for this proton (4.55 ppm) in the ^1H NMR spectrum, and confirms congruence between the solid state and solution state structures of the complex. The bimetallic structure may also be stabilized by a $\pi-\pi$ stacking interaction between the two pyrazole rings coordinated *trans* to CO ($C3A-pyrazole_{centroid}$ = 3.450 Å).

Structural Dynamics of 8, 9, 10, 13, and 14 in Solution. In the ^1H and ^{13}C NMR spectra of complexes **8**, **9**, **10**, **13**, and **14** a highly fluxional coordination environment is evident. For example, a strong exchange correlation peak (EXSY) between resonances due to the diastereotopic methylene protons (CH^aH^b) of the NCN ligands in complexes **8** and **10** indicates these protons are exchanging environments during the signal acquisition. An exchange correlation was also observed between the resonances due to the axial and equatorial COD alkene protons of **8** and **9**. In the ^1H NMR spectrum of complex **10**, the COD alkene protons are not observed at 298 K due to extreme line broadening but resolve from the spectrum baseline at 248 K (δ 4.98 and 2.76 ppm, 400 MHz, acetone-d_6). This behavior is also consistent with exchange of the COD axial and equatorial positions. In the ^1H NMR of the corresponding dicarbonyl complexes **13** and **14** the geminal methylene protons (CH^aH^b) were equivalent, indicating rapid exchange between H^a and H^b. Diastereotopic splitting of these resonance pairs was only observed at low temperature (~193 K). The axial and equatorial CO ligands also undergo rapid exchange at room temperature with the ^{13}C NMR spectra containing a single doublet resonance for the two CO ligands of the Rh complex **13** (185.4 ppm, $^1J_{Rh-C}$ = 55.6 Hz) and a highly broadened singlet for the two CO ligands of the Ir complex **14** (181.6 ppm, peak width at half-maximum = 120 Hz).

These spectral features indicate that the trigonal bipyramidal complexes **8**, **9**, **10**, **13**, and **14** are undergoing conformational exchange between two mirror-image isomers (**A** and **B**) as shown in Figure 6. To determine at what relative rate this exchange was occurring, we determined the temperature at which exchange induced line broadening became significant in the ^1H NMR spectra of the complexes. For example, as discussed above, the resonances due to the COD alkene protons of complex **10** are broadened beyond the baseline resolution of the spectrum at 298 K. For complex **8** the COD alkene resonances only broaden beyond the baseline resolution at 338 K, while for complex **9** the same resonances remained sharp up to 348 K. This would indicate the exchange rates

dx.doi.org/10.1021/ic501158x | *Inorg. Chem.* 2014, 53, 10159−10170

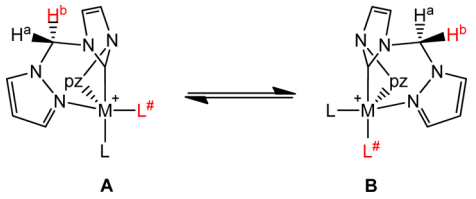

Figure 6. Conformational exchange observed for complexes **8**, **9**, **10**, **13**, and **14**.

follow the order **10** > **8** > **9**. Meanwhile, for complexes **13** and **14** the rapid exchange of the methylene proton resonances (CH^aH^b) would indicate that isomers **A** and **B** of the dicarbonyl complexes are exchanging at a faster rate than those of the COD containing analogues **9** and **10**. Such a rate order is consistent with a Berry pseudorotational mechanism where the transition is accelerated by the monodentate CO coligands (**9** and **10**, cf. **13** and **14**) and a larger Ir ion (**8** cf. **10**).

Catalysis Studies. The Ir and Rh complexes **8**, **9**, **10**, **13**, **14**, and **15** were investigated as catalysts for several different reactions involving the addition of an X−H bond across an unsaturated carbon−carbon triple bond. The reactions taken into consideration were hydroamination (N−H), hydrocarboxylation (O−H), and hydrosilylation (Si−H). For comparison we also included the previously reported[17] complexes [Rh(NC)(COD)]BPh_4 (**16**) and [Rh(NC)(CO)]-BPh_4 (**17**) which contain a bidentate NHC−pyrazolyl ligand (NC) in these catalytic studies (Figure 7). Due to the instability

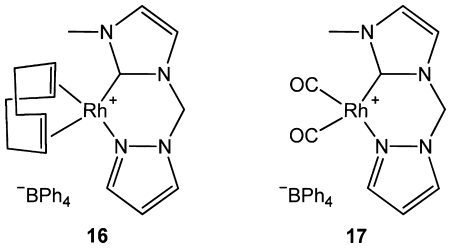

Figure 7. Previously reported complexes **16** and **17** included in the catalytic studies.

of the CO containing complexes **13** and **14**, all CO containing catalysts (**13**, **14**, **15**, and **17**) were generated in situ from the corresponding COD complexes by performing the catalyzed reaction under 1 atm of carbon monoxide. For the bimetallic catalyst **15** catalyst loadings were calculated per Rh center to give equal metal concentrations for both monometallic and bimetallic catalyzed reactions.

Hydroamination of 5-Phenyl-4-pentyn-1-amine (18). The intramolecular hydroamination of 5-phenyl-4-pentyn-1-amine (**18**) to 2-benzyl-1-pyrroline (**19**) was carried out at 100 °C in dioxane-d_8 using 5 mol % catalyst, and the reaction progress was monitored using ^{1}H NMR spectroscopy. Relative conversions of substrate to product obtained after 12 h are shown in Table 1. For the catalysts **8**, **9**, **10**, and **16** containing a COD coligand, poor overall catalyst efficiency was obtained, with the Ir complex **10** achieving the highest conversion to product of all catalysts with only 55% conversion in 12 h. In the case of the Rh complexes, a bidentate ligand coordination appeared to be more beneficial for catalyst efficiency with complex **16** (40% conversion) outperforming complexes **8** and **9** (23 and 33% conversion, respectively) that each contain a

Table 1. Cyclization of 5-Phenyl-4-pentyn-1-amine (18)[a]

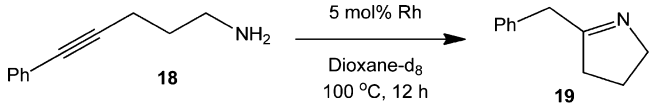

catalyst	conv[b] (%)	catalyst[c]	conv[b] (%)
[Ir(NCN^{me})(COD)] BPh_4 (**10**)	55	[Ir(NCN^{me})$(CO)_2$]BPh_4 (**14**)	37
[Rh(NCN^{me})(COD)] BPh_4 (**8**)	23	[Rh(NCN^{me}) $(CO)]_2(BPh_4)_2$ (**15**)	83
[Rh(NCN^{et})(COD)] BPh_4 (**9**)	33	[Rh(NCN^{et})$(CO)_2$]BPh_4 (**13**)	69
[Rh(NC)(COD)]BPh_4 (**16**)	40	[Rh(NC)$(CO)_2$]BPh_4 (**17**)	100

[a]Reaction carried out in 1,4-dioxane-d_8 at 100 °C using 5 mol % Rh. [b]Conversions were determined by comparison of the product and substrate integrals in the ^{1}H NMR spectra of the reactions and are reported after 12 h. [c]Reactions with these catalysts were performed under an atmosphere of CO to generate the catalyst in situ from the corresponding COD containing complexes.

tridentate ligand. Complex **9**, which contains more labile pyrazole groups compared to those of **8**, shows an intermediate level of catalytic activity between complex **16** and complex **8**. This would suggest that the hemilabile dissociation of a pyrazole donor during reaction is responsible for the increased catalytic efficiency of complex **9** compared to that of complex **8**.

In the case of the Rh complexes containing CO coligands, the bidentate ligand coordination of complex **17** (with 100% conversion of substrate) is again more advantageous than the tridentate ligand coordination of **13** (with only 69% conversion). In general the CO containing Rh catalysts are much more efficient than their COD containing counterparts, with the bimetallic complex **15** (83% substrate conversion) also proving to be an effective catalyst for this reaction. In contrast, the Ir complex **14** (37% substrate conversion) was the least active catalyst of the CO containing series and was less active than its COD containing analogue **10** (Table 1).

We have previously investigated the hydroamination of **18** using analogous [Rh(L)$(CO)_2$]BPh_4 and [Ir(L)$(CO)_2$]BPh_4 complexes containing the bidentate N-donor ligands bis(1-pyrazolyl)methane (bpm) or bis(*N*-methyl-2-imidazolyl)-methane (bim) as L.[18] These previously reported rhodium complexes were more active catalysts for hydroamination than the NHC containing catalysts reported here. Under similar reaction conditions (dioxane-d_8, 95 °C, 5 mol % catalyst) the catalyst [Rh(bpm)$(CO)_2$]BPh_4 achieved 87% conversion in 4.5 h and [Rh(bim)$(CO)_2$]BPh_4 achieved 96% conversion in 2.3 h. The previously reported iridium complexes were much less effective catalysts than their Rh analogues, with [Ir(bpm)-$(CO)_2$]BPh_4 and [Ir(bim)$(CO)_2$]BPh_4 obtaining 92 and 32% conversion, respectively, within 49 h. This parallels the reactivity trend observed here with the CO containing catalysts **13**−**15**.

Hydrocarboxylation of 4-Pentynoic acid (20). To explore the efficiency of complexes **8**, **9**, **10**, **13**, **14**, **15**, **16**, and **17** as catalysts for the addition of OH bonds to alkynes, we investigated the catalyzed cyclization of 4-pentynoic acid (**20**) to form γ-methylene-γ-butyrolactone (**21**). The reaction was performed in THF-d_8 at 80 °C for 24 h, and the reaction progress was monitored periodically by ^{1}H NMR spectroscopy (Figure 8). Figure 8a shows the reaction profiles for complexes **8**, **9**, **10**, and **16**, which contain a COD coligand. The most

dx.doi.org/10.1021/ic501158x | Inorg. Chem. 2014, 53, 10159−10170

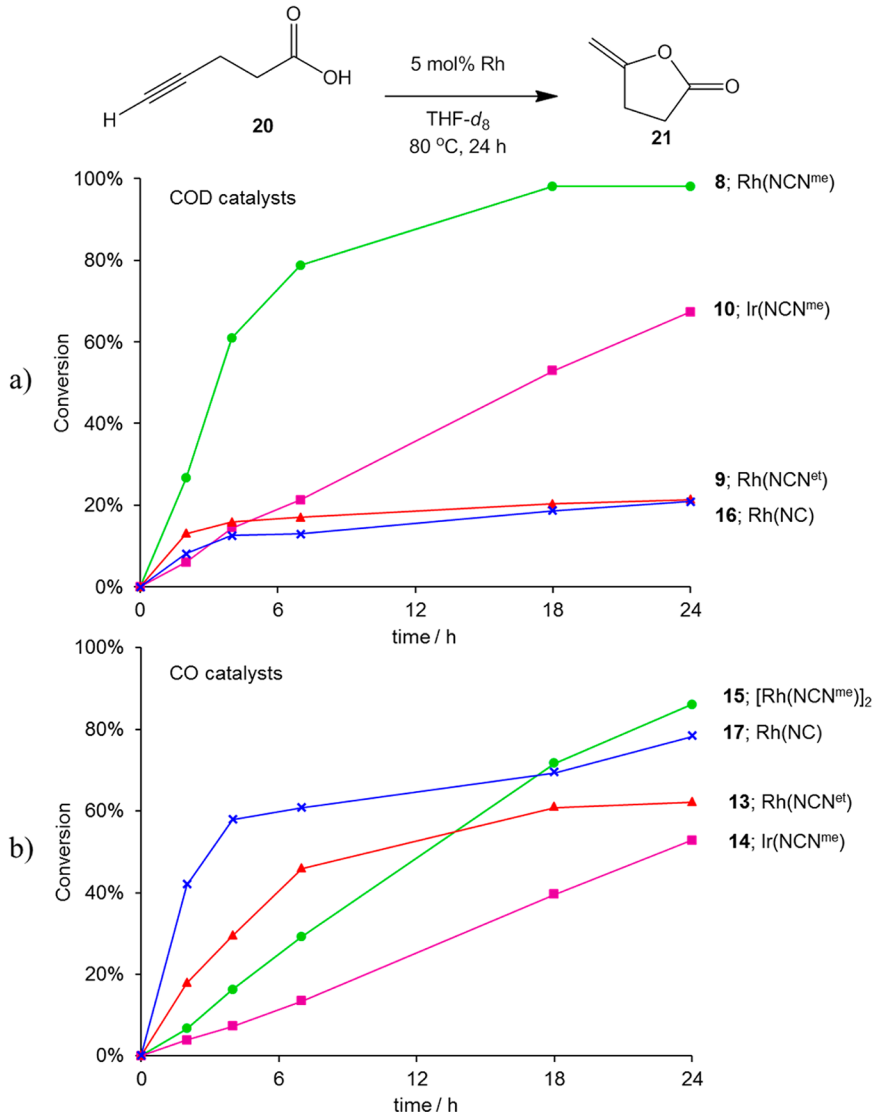

Figure 8. Catalyzed hydrocarboxylation of 4-pentynoic acid (**20**) using catalysts with (a) COD coligands and (b) CO coligands.

active catalyst of this series was [Rh(NCN^{me})(COD)]BPh$_4$ (**8**), achieving complete conversion of the substrate after 18 h. In comparison, [Rh(NCN^{et})(COD)]BPh$_4$ (**9**) and [Rh(NC)(COD)]BPh$_4$ (**16**) both achieved a maximum conversion of only 21% due to a rapid deactivation of the catalyst within the first few hours of reaction. The rapid deactivation of the catalysts **9** and **16** could be attributed to the absence of a strongly coordinating third donor arm, with a high degree of lability of the pyrazole donors in **9** and no third donor arm in **16**. In contrast, the strong tridentate coordination of the NCN^{me} ligand in **8** appears to stabilize the catalyst during reaction. The Ir catalyst [Ir(NCN^{me})(COD)]BPh$_4$ (**10**) was moderately effective, achieving 67% conversion after 24 h with no apparent signs of catalyst deactivation.

The reaction profiles for catalysts **13**, **14**, **15**, and **17** containing CO coligands as catalysts for the hydrocarboxylation reaction are shown in Figure 8b. The activity of [Rh(NCN^{et})(CO)$_2$]BPh$_4$ (**13**) and and that of [Rh(NC)(CO)$_2$]BPh$_4$ (**17**) for the hydrocarboxylation reaction were dramatically increased compared to those of the isostructural catalysts **9** and **16** containing COD coligands. Despite a very fast initial reaction rate both catalysts **13** and **17** deactivate after several hours of reaction, obtaining final conversions of only 62 and 78%, respectively. In contrast, the bimetallic catalyst [Rh(NCN^{me})(CO)]$_2$(BPh$_4$)$_2$ (**15**) remained active throughout the reaction, resulting in a higher conversion after 24 h of 86%. The Ir catalyst [Ir(NCN^{me})(CO)$_2$]BPh$_4$ (**14**) proved the least effective of this series (53%, 24 h) and was also less effective than its isostructural COD containing analogue, **10**.

The catalyzed hydrocarboxylation reaction has been proposed to proceed via oxidative addition of the acid OH group to Rh(I) as a first step.[19] The increased stability afforded to the resulting Rh(III) hydride intermediate may explain why a tridentate ligand coordination is beneficial for the hydrocarboxylation reaction. On the other hand, the catalyst remains in the +1 oxidation state throughout the rhodium catalyzed hydroamination reaction, for which a tridentate coordination appears *not* to be necessary for stability or reactivity.[18] In contrast to the results obtained above, related rhodium complexes containing bidentate ligand groups have proven highly effective at catalyzing the hydrocarboxylation of 4-pentynoic acid (**20**). Using 0.5 mol % of the catalyst [Rh(L)(COD)]Cl, where L is a bidentate NHC−pyridine ligand, Peris and co-workers reported the complete conversion

dx.doi.org/10.1021/ic501158x | *Inorg. Chem.* 2014, 53, 10159−10170

of **20** within 12 h at 50 °C, with no apparent sign of catalyst decomposition.[20] Other Rh(I) catalysts that have proven effective for this transformation include $[Rh(dcpe)Cl]_2$ (93% conversion in 24 h, 2 mol % catalyst at 25 °C; dcpe = 1,2-bis(dicyclohexylphospino)ethane)[19a] and $[Rh(bim)(CO)_2]BPh_4$ (88% conversion in 16 h, 0.4 mol % catalyst at 50 °C; bim = bis(*N*-methyl-2-imidazolyl)methane).[19b]

Hydrosilylation of 1-Phenylpropyne (22) and Phenylacetylene (24). The hydrosilylation of 1-phenylpropyne (**22**) with triethylsilane to form the regioisomeric products **23**-*β*-*E* and **23**-*β*-*Z* was investigated using complexes **8**, **10**, **14**, and **15** as catalysts (Figure 9a). The reactions were performed in

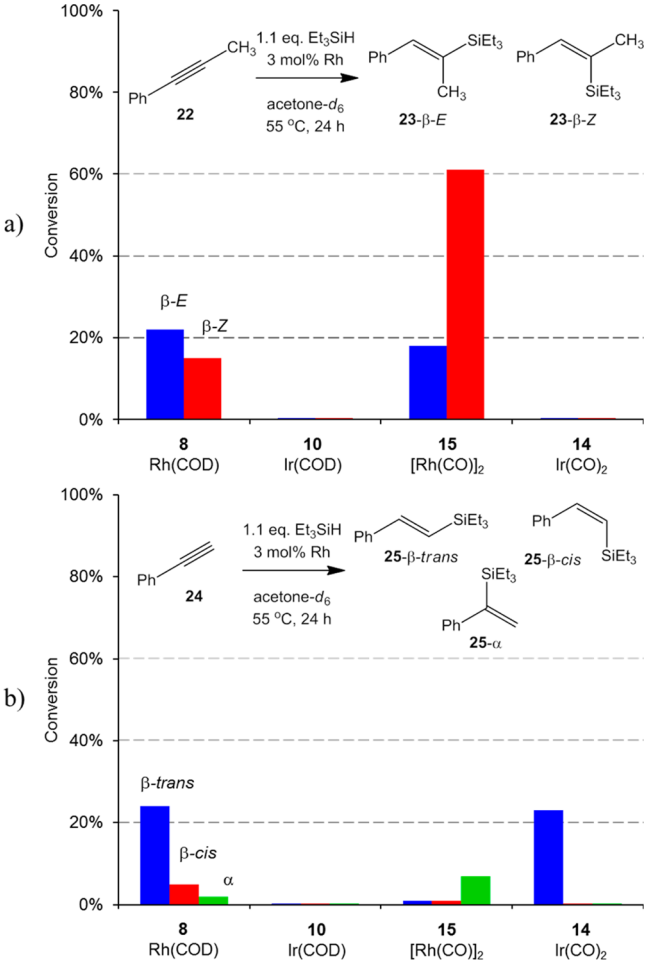

Figure 9. Catalyzed hydrosilylation of (a) 1-phenylpropyne (**22**) and (b) phenylacetylene (**24**) with triethylsilane using catalysts containing the NCN^{me} ligand.

acetone-d_6 at 55 °C for 24 h using 1.1 equiv of Et_3SiH and 3 mol % Rh. The catalyst $[Rh(NCN^{me})(COD)]BPh_4$ (**8**) achieved a total conversion of 37% but showed poor selectivity between *E* and *Z* isomers (**23**-*β*-*E*:**23**-*β*-*Z* = 22:15). The bimetallic catalyst $[Rh(NCN^{me})(CO)]_2(BPh_4)_2$ (**15**) was more effective, achieving a total conversion to both products of 79% with a high level of selectivity for the *β*-*Z* isomer (**23**-*β*-*E*:**23**-*β*-*Z* = 18:61). In contrast, both Ir catalysts $[Ir(NCN^{me})(COD)]BPh_4$ (**10**) and $[Ir(NCN^{me})(CO)_2]BPh_4$ (**14**) were entirely inactive for this reaction.

The hydrosilylation of phenylacetylene (**24**) with triethylsilane afforded three regioisomeric products; **25**-*β*-*trans*, **25**-*β*-*cis*, and **25**-*α* (Figure 9b). This reaction was performed under conditions identical to those of the hydrosilylation of 1-phenylpropyne (**22**) using complexes **8**, **10**, **14**, and **15** as catalysts. All complexes displayed a very low activity as catalysts for the hydrosilylation of phenylacetylene. Complex $[Rh(NCN^{me})(COD)]BPh_4$ (**8**) promoted the reaction with a total conversion of only 31% and a high selectivity for the *β*-*trans* product (**25**-*β*-*trans*:*β*-*cis*:*α* = 24:5:2). The analogous Ir complex $[Ir(NCN^{me})(COD)]BPh_4$ (**10**) in comparison was entirely inactive (<1% conversion). Substituting the COD coligand in **10** for CO gave the more active catalyst $[Ir(NCN^{me})(CO)_2]BPh_4$ (**14**), which was exclusively selective for the **25**-*β*-*trans* isomer (23% conversion). The bimetallic catalyst $[Rh(NCN^{me})(CO)]_2(BPh_4)_2$ (**15**) only obtained a total conversion of 9%, but intriguingly the reaction was highly selective for the *α* isomer (**25**-*β*-*trans*:*β*-*cis*:*α* = 1:1:7), which is seldom favored in rhodium catalyzed hydrosilylation reactions.[1f]

The hydrosilylation of alkynes catalyzed by Rh complexes that contain a bidentate ligand incorporating one NHC donor group and one N-donor group (e.g., pyridine,[20] oxazole,[21] amine,[22] or carboxamide[23]) has been reported previously by several groups. The reactions typically proceed to give quantitative conversion of the substrate within 24 h under reaction conditions comparable to those employed here. This would suggest a tridentate coordination of the NCN^{me} ligand as used here inhibits the hydrosilylation activity of the Rh and Ir complexes with relatively low conversions. Interestingly, a tridentate coordination of NHC containing pincer ligands has previously afforded highly active hydrosilylation catalysts with Rh in the +3 oxidation state.[6a,14d]

■ CONCLUSIONS

The two pincer ligands NCN^{me} and NCN^{et} were found to have a surprisingly diverse coordination chemistry with Rh(I) and Ir(I). Four distinct coordination modes were crystallographically characterized including tridentate (complexes **8** and **10**), bidentate (complex **9**), and monodentate (complexes **11** and **12**) coordination plus an unusual bimetallic bridging mode (complex **15**). Increasing the length of the alkyl chain between the NHC and pyrazole donors from methylene in NCN^{me} to ethylene in NCN^{et} was found to increase the lability of the pyrazole groups. This resulted in both tridentate and bidentate NCN^{et} coordination being characterized for complex **9**, in the solution and solid state respectively, indicating the potential for hemilabile coordination of the ligand.

The complexes developed in this work were shown to be effective catalysts for the addition of NH and OH bonds to the unsaturated C−C bond of alkynes. They were also shown to be poor catalysts for the addition of SiH bonds to the unsaturated C−C bond of alkynes. In comparison to previously reported complexes **16** and **17** which contain a bidentate NHC−pyrazole ligand, the inclusion of a tridentate NCN ligand in complexes **8**, **9**, and **13** was found to inhibit the efficiency of the catalyzed hydroamination of 5-phenyl-4-pentyn-1-amine (**18**) and enhance the efficiency of the catalyzed hydrocarboxylation of 4-pentynoic acid (**20**). The large difference in catalytic activity of complex **8** compared to complex **9** also indicated that hemilabile coordination of the NCN^{et} ligand in **9** has a substantial impact on the reactivity of the complex.

■ EXPERIMENTAL SECTION

All manipulations of metal complexes and air-sensitive reagents were carried out using standard Schlenk techniques or in a nitrogen-filled

dx.doi.org/10.1021/ic501158x | Inorg. Chem. 2014, 53, 10159−10170

Table 2. Crystallographic Data for Compounds 8−12 and 15

	8	9	10	11	12	15
chem formula	$C_{43}H_{44}BN_6Rh\cdot1.25(CH_2Cl_2)$	$C_{45}H_{48}BN_6Rh$	$C_{43}H_{44}BIrN_6\cdot C_4H_8O$	$C_{54}H_{56}BIrN_{12}\cdot0.5(CH_2Cl_2)$	$C_{58}H_{64}BIrN_{12}\cdot CH_2Cl_2$	$C_{72}H_{64}B_2N_{12}O_2Rh_2\cdot C_3H_6O$
M_r (g/mol)	864.72	786.61	919.95	1118.58	1217.15	707.44
cryst syst, space group	monoclinic, $P2_1/n$	monoclinic, $P2_1$	monoclinic, $P2_1/c$	triclinic, $P\bar{1}$	monoclinic, $P2_1$	monoclinic, $P2_1/n$
temp (K)	156	180	163	293	150	150
a, b, c (Å)	17.425(3), 11.8512(16), 21.719(3)	11.6656(3), 11.3435(3), 14.6475(4)	11.8066(4), 9.6104(3), 35.9142(11)	10.3367(3), 12.8201(4), 19.6142(7)	11.0074(11), 24.210(2), 11.3930(11)	12.6272(4), 26.3368(8), 22.9366(7)
β (deg)	108.686(5)	97.391(1)	95.944(2)	α = 92.847(1), β = 102.154(2), γ = 94.312(1)	113.011(2)	91.129(1)
V (Å^3)	4248.8(11)	1922.18(9)	4053.1(2)	2528.05(14)	2794.5(5)	7626.3(4)
Z	4	2	4	2	2	8
μ (mm^{-1})	0.57	0.49	3.34	2.8	2.54	0.48
cryst size (mm)	0.33 × 0.30 × 0.09	0.36 × 0.17 × 0.09	0.17 × 0.13 × 0.05	0.36 × 0.29 × 0.21	0.27 × 0.26 × 0.10	0.13 × 0.09 × 0.07
T_{min}, T_{max}	0.837, 0.950	0.846, 0.960	0.599, 0.840	0.432, 0.591	0.545, 0.779	0.939, 0.968
no. of measd, independent, and obsd $[I > 2\sigma(I)]$ reflns	29 496, 7459, 6533	14 078, 6146, 5963	27 051, 7108, 5974	35 831, 8907, 8566	31 734, 9695, 9460	80 179, 13 379, 6866
R_{int}	0.032	0.026	0.037	0.027	0.029	0.115
$(\sin\theta/\lambda)_{max}$ (Å^{-1})	0.595	0.595	0.595	0.595	0.595	0.595
R $[F^2 > 2\sigma(F^2)]$, $wR(F^2)$, S	0.038, 0.119, 1.04	0.021, 0.055, 1.04	0.028, 0.059, 1.05	0.025, 0.066, 1.05	0.016, 0.040, 1.00	0.065, 0.194, 1.03
no. of params, restraints	533, 0	478, 1	505, 0	641, 0	712, 73	884, 39
$\Delta\rho_{max}$, $\Delta\rho_{min}$ (e Å^{-3})	0.86, −0.47	0.33, −0.22	0.77, −1.11	1.21, −1.56	0.38, −0.59	0.75, −0.46

dx.doi.org/10.1021/ic501158x | Inorg. Chem. 2014, 53, 10159−10170

Braun glovebox. Reagents were purchased from Aldrich Chemical Co. Inc. or Alfa Aesar Inc. and were used without further purification unless otherwise stated. Iridium(III) chloride hydrate and rhodium(III) chloride hydrate were obtained from Precious Metals Online, PMO P/L. Isotopically enriched ^{13}CO (>99.5%) and all deuterated solvents were obtained from Cambridge Isotopes Laboratories. Tetrahydrofuran (THF), diethyl ether, *n*-pentane, and toluene were obtained from a PuraSolv solvent purification system, dichloromethane (DCM) was distilled from calcium hydride, and methanol was distilled from dimethoxymagnesium prior to use. Deuterated solvents were distilled under vacuum from sodium benzophenone ketyl radical (THF-d_8 and dioxane-d_8) or calcium sulfate (acetone-d_6). The catalyst substrates 1-phenylpropyne (**22**) and phenylacetylene (**24**) were distilled under vacuum and stored over 4 Å molecular sieves. 1-(hydroxymethyl)pyrazole,[24] 1-(2-bromoethyl)pyrazole,[25] $[Rh(\mu\text{-Cl})(COD)]_2$,[26] $[Ir(\mu\text{-Cl})(COD)]_2$,[27] $[Rh(NC)(COD)]BPh_4$ (**16**),[17] $[Rh(NC)(CO)_2]BPh_4$ (**17**),[17] and 5-phenyl-4-pentyn-1-amine (**18**)[28] were synthesized using reported methods. ^1H and $^{13}C\{^1H\}$ NMR spectra were recorded on Bruker DPX300, DMX400, and DMX600 spectrometers at 298 K unless otherwise specified. Chemical shifts (δ) are quoted in parts per million and referenced to internal solvent resonances. The abbreviations *pz* (pyrazole) and *im* (imidazole) are used to identify NMR signals. Infrared spectra were measured using a Nicolet 380 Avatar FTIR spectrometer. Elemental analyses were carried out at the Campbell Microanalytical Laboratory, University of Otago, New Zealand, and the Elemental Analysis Unit, Australian National University, Canberra. Single crystal X-ray analyses were carried out at the Mark Wainwright Analytical Centre, University of New South Wales, Sydney. X-ray diffraction measurements were carried out on a Bruker kappa APEXII CCD diffractometer using graphite-monochromated Mo Kα radiation (λ = 0.710 723 Å) (Table 2). All structures were solved by direct methods, and the full-matrix least-squares refinements were carried out using SHELXL.[29] Absorption correction was performed using Multiscan SADABS, and H atom parameters were treated as constrained.

Synthesis of $NCN^{me}.HBPh_4$ (6). 1-(hydroxymethyl)pyrazole (1.60 g, 16.3 mmol) was dissolved in 70 mL of chloroform, and an excess of thionyl chloride (5 mL, ~70 mmol) was added slowly over 1 min. The solution was refluxed overnight and the volatiles were removed under vacuum to form a residue of 1-(chloromethyl)pyrazole hydrochloride in quantitative yield.[30] (Note: 1-(Chloromethyl)pyrazole hydrochloride cannot be isolated as its free base and undergoes hydrolysis back to 1-(hydroxymethyl)pyrazole in the presence of atmospheric water.) The residue of 1-(chloromethyl)pyrazole hydrochloride was suspended in dry toluene (70 mL), trimethylsilyl imidazole (1.2 mL, 8.2 mmol) was added, and the mixture was refluxed overnight to give a viscous brown oil. The toluene was decanted and the oil was dissolved in methanol (160 mL); addition of $NaBPh_4$ (2.8 g, 8.2 mmol) resulted in the precipitation of $NCN^{me}{\cdot}HBPh_4$ (**6**) as a white powder which was filtered, washed with methanol (70 mL), and dried in vacuo. Yield: 1.89 g (42%). Analysis found (calculated for $C_{35}H_{33}BN_6$): C, 76.34 (76.64); H, 6.16 (6.06); N, 15.07 (15.32). ^1H NMR (400 MHz, dmso-d_6): δ 9.62 (t, ^4J = 1.5 Hz, 1H, NC*H*N), 8.10 (d, ^3J = 2.4 Hz, 2H, *pz*-NC*H*), 7.84 (d, ^3J = 1.4 Hz, 2H, *im*-C*H*C*H*), 7.65 (d, ^3J = 1.3 Hz, 2H, *pz*-NC*H*), 7.20 (m, 8H, *o*-BPh_4), 6.94 (t, ^3J = 7.3 Hz, 8H, *m*-BPh_4), 6.80 (t, ^3J = 7.2 Hz, 4H, *p*-BPh_4), 6.58 (s, 4H, CH_2), 6.40 (t, ^3J = 2.0 Hz, 2H, *pz*-NCHC*H*). $^{13}C\{^1H\}$ NMR (100 MHz, dmso-d_6): δ 163.4 (q, ^1J(BC) = 49.7 Hz, B*C*), 141.8 (*pz*-NCH), 136.9 (NCHN), 135.6 (*o*-BPh_4), 131.7 (*pz*-NCH), 125.3 (*m*-BPh_4), 122.4 (*im*-CHCH), 121.6 (*p*-BPh_4), 107.2 (*pz*-NCHCH), 61.6 (CH_2).

Synthesis of $NCN^{et}{\cdot}HBPh_4$ (7). 1-(2-Bromoethyl)pyrazole (3.20 g, 18.3 mmol) was dissolved in dry toluene (70 mL), trimethylsilyl imidazole (1.30 g, 9.1 mmol) was added, and the solution was refluxed overnight. A brown oil precipitated and the toluene was decanted. The oil was dissolved in methanol (100 mL) and $NaBPh_4$ (3.10 g, 9.1 mmol) was added, resulting in the precipitation of $NCN^{et}{\cdot}HBPh_4$ (**7**) as a white powder which was filtered, washed with methanol (70 mL), and dried in vacuo. Yield: 3.80 g (72%). Analysis found (calculated for $C_{37}H_{37}BN_6$): C, 77.46 (77.08); H, 6.54 (6.47); N, 14.37 (14.58). ^1H NMR (400 MHz, dmso-d_6): δ 8.72 (t, ^4J = 1.4 Hz, 1H, NC*H*N), 7.54 (d, ^3J = 2.0 Hz, 2H, *pz*-NC*H*), 7.47 (d, ^3J = 1.3 Hz, 2H, *pz*-NC*H*), 7.41 (d, ^3J = 1.4 Hz, 2H, *im*-C*H*C*H*), 7.19 (m, 8H, *o*-BPh_4), 6.93 (t, ^3J = 7.4 Hz, 8H, *m*-BPh_4), 6.79 (t, ^3J = 7.2 Hz, 4H, *p*-BPh_4), 6.23 (t, ^3J = 2.0 Hz, 2H, *pz*-NCHC*H*), 4.55 (m, 8H, CH_2). $^{13}C\{^1H\}$ NMR (100 MHz, dmso-d_6): δ 163.4 (q, ^1J(BC) = 49.3 Hz, B*C*), 139.7 (*pz*-NCH), 136.7 (NCHN), 135.5 (*o*-BPh_4), 130.6 (*pz*-NCH), 125.3 (*m*-BPh_4), 122.5 (*im*-CHCH), 121.5 (*p*-BPh_4), 105.7 (*pz*-NCHCH), 50.4 (CH_2), 49.0 (CH_2).

Synthesis of $[Rh(NCN^{me})(COD)]BPh_4$ (8). The imidazolium salt $NCN^{me}.HBPh_4$ (**6**, 0.175 g, 0.32 mmol), $[Rh(\mu\text{-Cl})(COD)]_2$ (0.093 g, 0.16 mmol), and sodium ethoxide (0.110 g, 1.6 mmol) were suspended in THF (30 mL), and the mixture was stirred for 2 h at room temperature. The solvent was then removed under vacuum and the residue was redissolved in dichloromethane (20 mL). After stirring for 30 min the resulting cloudy yellow solution was filtered and pentane (15 mL) was added to precipitate $[Rh(NCN^{me})(COD)]BPh_4$ (**8**) as a yellow powder which was filtered and dried in vacuo. Yield: 0.187 g (77%). Electrospray ionization high-resolution mass spectrometry (ESI-HRMS) found (calculated): *m*/*z* 439.1110 ($[M]^+$, 439.1112). ^1H NMR (400 MHz, dmso-d_6): δ 8.01 (m, 4H, *pz*-NC*H*), 7.44 (s, 2H, *im*-C*H*C*H*), 7.17 (m, 8H, *o*-BPh_4), 6.92 (t, ^3J = 7.4 Hz, 8H, *m*-BPh_4), 6.78 (t, ^3J = 7.2 Hz, 4H, *p*-BPh_4), 6.63 (br s, 2H, NC*H*^{a}H^b), 6.38 (t, ^3J = 2.1 Hz, 2H, *pz*-NCHC*H*), 6.36 (br s, 2H, NCH^a*H*^{b}), 5.19 (br s, 2H, COD C*H*), 3.10 (br s, 2H, COD C*H*), 2.40 (br s, 2H, COD CH_2), 2.16 (br s, 2H, COD CH_2), 1.96 (br s, 4H, COD CH_2). $^{13}C\{^1H\}$ NMR (100 MHz, dmso-d_6): δ 184.0 (d, ^1J(RhC) = 43.7 Hz, NCN), 163.4 (q, ^1J(BC) = 49.4 Hz, B*C*), 142.1 (*pz*-NCH), 135.5 (*o*-BPh_4), 132.2 (*pz*-NCH), 125.3 (*m*-BPh_4), 122.0 (*im*-CHCH), 121.5 (*p*-BPh_4), 106.8 (*pz*-NCHCH), 103.3 (COD CH), 62.5 (NCH_2), 51.7 (d, ^1J(RhC) = 16.2 Hz, COD CH), 34.0 (COD CH_2), 28.2 (COD CH_2).

Synthesis of $[Rh(NCN^{et})(COD)]BPh_4$ (9). The imidazolium salt $NCN^{et}.HBPh_4$ (**7**, 0.266 g, 0.46 mmol), $[Rh(\mu\text{-Cl})(COD)]_2$ (0.114 g, 0.23 mmol), and sodium ethoxide (0.071 g, 1.1 mmol) were dissolved in methanol (20 mL), and the mixture was refluxed for 30 min and then stirred at room temperature overnight. A yellow precipitate of $[Rh(NCN^{et})(COD)]BPh_4$ (**9**) formed which was filtered and recrystallized from DCM/pentane. Yield: 0.203 g (56%). ESI-HRMS found (calculated): *m*/*z* 467.1424 ($[M]^+$, 467.1425). ^1H NMR (400 MHz, dmso-d_6): δ 7.64 (d, ^3J = 2.3 Hz, 2H, *pz*-NC*H*), 7.54 (d, ^3J = 2.0 Hz, 2H, *pz*-NC*H*), 7.17 (m, 10H, *o*-BPh_4 and *im*-C*H*C*H*), 6.92 (t, ^3J = 7.3 Hz, 8H, *m*-BPh_4), 6.78 (t, ^3J = 7.3 Hz, 4H, *p*-BPh_4), 6.27 (t, ^3J = 2.2 Hz, 2H, *pz*-NCHC*H*), 5.48 (m, 2H, NCH_2), 4.93 (m, 4H, NCH_2), 4.72 (br s, 2H, COD C*H*), 4.58 (m, 2H, NCH_2), 3.97 (br s, 2H, COD C*H*), 2.48 (m, 4H, COD CH_2), 2.03 (m, 4H, COD CH_2). $^{13}C\{^1H\}$ NMR (100 MHz, dmso-d_6): δ 175.0 (d, ^1J(RhC) = 52.3 Hz, NCN), 163.4 (q, ^1J(BC) = 49.4 Hz, B*C*), 140.1 (*pz*-NCH), 135.5 (*o*-BPh_4), 132.1 (*pz*-NCH), 125.3 (q, ^3J(BC) = 2.8 Hz, *m*-BPh_4), 122.9 (*im*-CHCH), 121.5 (*p*-BPh_4), 106.4 (*pz*-NCHCH), 95.5 (d, ^1J(RhC) = 7.4 Hz, COD CH), 76.0 (d, ^1J(RhC) = 12.6 Hz, COD CH), 51.0 (NCH_2), 49.6 (NCH_2), 31.8 (COD CH_2), 28.7 (COD CH_2).

Synthesis of $[Ir(NCN^{me})(COD)]BPh_4$ (10) and $[Ir(NCN^{me})_2(COD)]BPh_4$ (11). The imidazolium salt $NCN^{me}.HBPh_4$ (**6**) (0.310 g, 0.56 mmol), $[Ir(\mu\text{-Cl})(COD)]_2$ (0.190 g, 0.28 mmol) and sodium ethoxide (0.095 g, 1.4 mmol) were dissolved in methanol (30 mL), and the mixture was stirred for 2 h at room temperature. A pale yellow precipitate and orange solution formed. The precipitate was filtered and recrystallized from THF/diethyl ether to give a pale yellow powder of $[Ir(NCN^{me})(COD)]BPh_4$ (**10**). Reduction of the orange filtrate to dryness and recrystallization of the residue from DCM/pentane gave $[Ir(NCN^{me})_2(COD)]BPh_4$ (**11**) as an orange powder.

*$[Ir(NCN^{me})(COD)]BPh_4$ (**10**).* Yield: 0.210 g (46%). Analysis found (calculated for $C_{43}H_{44}BIrN_6$): C, 60.65 (60.84); H, 5.66 (5.34); N, 9.67 (9.90). ESI-HRMS found (calculated): *m*/*z* 529.1687 ($[M]^+$, 529.1686). ^1H NMR (400 MHz, dmso-d_6): δ 8.06 (d, ^3J = 2.3 Hz, 4H, *pz*-NC*H*), 7.46 (s, 2H, *im*-C*H*C*H*), 7.17 (m, 8H, *o*-BPh_4), 6.92 (t, ^3J = 7.4 Hz, 8H, *m*-BPh_4), 6.78 (t, ^3J = 7.2 Hz, 8H, *p*-BPh_4), 6.66 (d, ^2J = 13.4 Hz, 2H, NC*H*^{a}H^b), 6.48 (t, ^3J = 2.2 Hz, 2H, *pz*-NCHC*H*), 6.18 (d, ^2J = 13.4 Hz, 2H, NCH^a*H*^{b}), 2.13 (br s, 4H, COD CH_2), 1.82 (br s,

dx.doi.org/10.1021/ic501158x | *Inorg. Chem.* 2014, 53, 10159−10170

4H, COD CH_2). Note, COD HC=CH protons are not observed at 298 K due to extreme line broadening but resolve from the spectrum baseline at 248 K. ^{1}H NMR (400 MHz, acetone-d_6, 248 K): δ 4.98 (br s, 2H, COD CH), 2.76 (br s, 2H, COD CH). $^{13}C\{^1H\}$ NMR (100 MHz, dmso-d_6): δ 203.0 (NCN), 163.4 (q, ^1J(BC) = 51.4 Hz, BC), 142.5 (*pz*-NCH), 135.5 (*o*-BPh_4), 132.6 (*pz*-NCH), 125.3 (*m*-BPh_4), 121.5 (*p*-BPh_4 and *im*-CHCH), 107.3 (*pz*-NCHCH), 62.9 (NCH_2), 42.7 (br s, COD CH_2). Note, HC=CH carbons are not observed at 298 K due to extreme line broadening.

*[Ir(NCN^{me})$_2$(COD)]BPh$_4$ (**11**).* Yield: 0.072 g (12%). ESI-MS: *m*/*z* 758.28 ([M]$^+$, 100%). ^{1}H NMR (400 MHz, dmso-d_6): δ 8.06 (d, ^3J = 2.2 Hz, 4H, *pz*-NC*H*), 7.62 (d, ^3J = 1.5 Hz, 4H, *pz*-NC*H*), 7.18 (m, 8H, *o*-BPh_4), 7.17 (s, 4H, *im*-C*H*CH), 6.95 (d, ^2J = 13.4 Hz, 4H, NC*H*^{a}H^b), 6.92 (m, 8H, *m*-BPh_4), 6.79 (t, ^3J = 7.1 Hz, 4H, *p*-BPh_4), 6.51 (d, ^2J = 13.4 Hz, 4H, NCH^a*H*^{b}), 6.41 (t, ^3J = 2.0 Hz, 4H, *pz*-NCHC*H*), 4.37 (br s, 4H, COD C*H*), 2.42 (br s, 4H, COD CH_2), 1.96 (br s, 4H, COD CH_2). $^{13}C\{^1H\}$ NMR (100 MHz, dmso-d_6): δ 177.0 (NCN), 163.4 (q, ^1J(BC) = 49.2 Hz, BC), 141.3 (*pz*-NCH), 135.5 (*o*-BPh_4), 132.0 (*pz*-NCH), 125.3 (q, ^3J(BC) = 2.6 Hz, *m*-BPh_4), 121.5 (*p*-BPh_4), 121.4 (*im*-CHCH), 106.5 (*pz*-NCHCH), 78.6 (COD CH), 64.2 (NCH_2), 30.8 (COD CH_2).

Synthesis of [Ir(NCN^{et})$_2$(COD)]BPh$_4$ (12). Sodium ethoxide (0.088 g, 1.3 mmol), [Ir(μ-Cl)(COD)]$_2$ (0.094 g, 0.14 mmol), and NCN^{et}·HBPh$_4$ (**7**) (0.310 g, 0.54 mmol) were dissolved in methanol (10 mL) and stirred for 1 h at room temperature. The solution was filtered and a precipitate was obtained by the addition of diethyl ether; this was recrystallized from THF/diethyl ether to afford [Ir(NCN^{et})$_2$(COD)]BPh$_4$ (**12**). Yield: 0.026 g (16%). ESI-MS: *m*/*z* 813.34 ([M]$^+$, 100%). ^{1}H NMR (600 MHz, dmso-d_6): δ 7.48 (d, ^3J = 2.0 Hz, 4H, *pz*-NC*H*), 7.45 (d, ^3J = 1.6 Hz, 4H, *pz*-NC*H*), 7.40 (s, 4H, *im*-C*H*CH), 7.17 (m, 8H, *o*-BPh_4), 6.92 (t, ^3J = 7.4 Hz, 8H, *m*-BPh_4), 6.78 (t, ^3J = 7.1 Hz, 4H, *p*-BPh_4), 6.22 (t, ^3J = 2.0 Hz, 4H, *pz*-NCHC*H*), 4.88 (m, 4H, NCH_2), 4.63 (m, 8H, NCH_2), 4.32 (m, 4H, NCH_2), 2.89 (br s, 4H, COD CH), 2.03 (br s, 4H, COD CH_2), 1.61 (m, 4H, COD CH_2). $^{13}C\{^1H\}$ NMR (100 MHz, dmso-d_6): δ 176.9 (NCN), 163.4 (q, ^1J(BC) = 50.9 Hz, BC), 139.3 (*pz*-NCH), 135.5 (*o*-BPh_4), 130.2 (*pz*-NCH), 125.3 (*m*-BPh_4), 121.5 (*p*-BPh_4), 121.0 (*im*-CHCH), 105.7 (*pz*-NCHCH), 75.6 (COD CH), 50.4 (NCH_2), 49.9 (NCH_2), 30.8 (COD CH_2).

Preparation of [Rh(NCN^{et})(CO)$_2$]BPh$_4$ (13) and [Ir(NCN^{me})(CO)$_2$]BPh$_4$ (14) in Situ. In a Young's NMR tube 0.020 g of [Rh(NCN^{et})(COD)]BPh$_4$ (**9**) or [Ir(NCN^{me})(COD)]BPh$_4$ (**10**) was dissolved in acetone-d_6. The solution was degassed via two freeze–pump–thaw cycles and an atmosphere of CO was introduced to the head space. The solution was shaken vigorously for several minutes to give the corresponding carbonyl complexes **13** or **14** and free COD in quantitative conversion.

*[Rh(NCN^{et})(CO)$_2$]BPh$_4$ (**13**).* FTIR (acetone): 2091 (CO) and 2034 (CO) cm^{-1}. ^{1}H NMR (400 MHz, acetone-d_6): δ 7.65 (m, 4H, *pz*-NC*H*), 7.35 (m, 8H, *o*-BPh_4), 7.18 (s, 2H, *im*-NC*H*CH), 6.92 (t, ^3J = 7.3 Hz, 8H, *m*-BPh_4), 6.78 (t, ^3J = 7.3 Hz, 4H, *p*-BPh_4), 6.35 (t, ^3J = 2.2 Hz, 2H, *pz*-NCHC*H*), 5.11 (br s, 4H, NCH_2), 4.79 (t, ^3J = 5.8 Hz, 4H, NCH_2). $^{13}C\{^1H\}$ NMR (100 MHz, acetone-d_6): δ 185.4 (d, ^1J(RhC) = 55.6 Hz, CO), 142.5 (*pz*-NCH), 137.0 (*o*-BPh_4), 133.2 (*pz*-NCH), 126.0 (q, ^3J(BC) = 2.8 Hz, *m*-BPh_4), 124.8 (*im*-CHCH), 122.3 (*p*-BPh_4), 108.1 (*pz*-NCHCH), 52.0 (CH_2), 51.7 (CH_2).

*[Ir(NCN^{me})(CO)$_2$]BPh$_4$ (**14**).* FTIR (acetone): 2081 (s, CO) and 2013 (s, CO) cm^{-1}. ^{1}H NMR (400 MHz, acetone-d_6): δ 8.20 (d, ^3J = 2.4 Hz, 2H, *pz*-NC*H*), 7.98 (d, ^3J = 2.2, 2H, *pz*-NC*H*), 7.63 (s, 2H, *im*-C*H*CH), 7.34 (m, 8H, *o*-BPh_4), 6.92 (t, ^3J = 7.3 Hz, 8H, *m*-BPh_4), 6.77 (t, ^3J = 7.3 Hz, 4H, *p*-BPh_4), 6.70 (br s, 4H, CH_2), 6.55 (t, ^3J = 2.3 Hz, 2H, *pz*-NCHC*H*). $^{13}C\{^1H\}$ NMR (100 MHz, acetone-d_6): δ 181.6 (very br s, CO), 145.5 (*pz*-NCH), 137.1 (*o*-BPh_4), 134.3 (*pz*-NCH), 126.0 (d, ^3J(BC) = 2.8 Hz, *m*-BPh_4), 123.7 (*im*-CHCH), 122.3 (*p*-BPh_4), 108.7 (*pz*-NCHCH), 64.8 (CH_2). Note, the ^{13}CO signals cannot be observed using natural abundance CO; isotopically enriched ^{13}CO (99.5%) was therefore employed. Free COD: ^{1}H NMR (400 MHz, acetone-d_6): δ 5.51 (br s, 4H, COD C*H*), 2.33 (br s, 8H, COD CH_2). $^{13}C\{^1H\}$ NMR (100 MHz, acetone-d_6): δ 129.3 (COD C*H*), 28.6 (COD CH_2).

Synthesis of [Rh(NCN^{me})(CO)]$_2$(BPh$_4$)$_2$ (15). A solution of [Rh(NCN^{me})(COD)]BPh$_4$ (**8**) (0.100 g, 0.13 mmol) in THF (10 mL) was degassed via two freeze–pump–thaw cycles, and an atmosphere of carbon monoxide was introduced to the head space. After vigorous stirring for 20 min an orange precipitate of [Rh(NCN^{me})(CO)]$_2$(BPh$_4$)$_2$ (**15**) formed which was filtered, washed with pentane (20 mL), and dried in vacuo. Yield: 0.051 g (57%). ESI-HRMS found (calculated): *m*/*z* 359.0124 ([M]$^{2+}$, 359.0122). FTIR (attenuated reflectance): 1998 (s, CO) cm^{-1}. ^{1}H NMR (400 MHz, dmso-d_6): δ 8.76 (d, ^3J = 2.5 Hz, 2H, *pz*-NC*H*), 7.93 (d, ^3J = 1.9 Hz, 2H, *pz*-NC*H*), 7.81 (d, ^3J = 2.3 Hz, 2H, *pz*-NC*H*), 7.76 (d, ^3J = 1.9 Hz, 2H, *im*-C*H*CH), 7.68 (d, ^3J = 2.0 Hz, 2H, *im*-C*H*CH), 7.28 (d, ^2J = 13.8 Hz, 2H, C*H*^{a}H^b), 7.17 (m, 16H, *o*-BPh_4), 6.92 (m, 18H, *m*-BPh_4 and CH^a*H*^{b}), 6.78 (t, ^3J = 7.5 Hz, 8H, *p*-BPh_4), 6.67 (t, ^3J = 2.4 Hz, 2H, *pz*-NCHC*H*), 6.62 (d, ^2J = 13.8 Hz, 2H, C*H*^{a}H^b), 6.42 (d, ^2J = 13.5 Hz, 2H, CH^a*H*^{b}), 5.70 (t, ^3J = 2.4 Hz, 2H, *pz*-NCHC*H*), 4.55 (d, ^3J = 2.0 Hz, 2H, *pz*-NC*H*). $^{13}C\{^1H\}$ NMR (150 MHz, dmso-d_6): δ 163.4 (q, ^1J(BC) = 49.0 Hz, BC), 146.8 (*pz*-NCH), 140.1 (*pz*-NCH), 136.0 (*pz*-NCH), 135.6 (*o*-BPh_4), 133.0 (*pz*-NCH), 125.3 (*m*-BPh_4), 124.7 (*im*-CHCH), 121.5 (*p*-BPh_4), 120.1 (*im*-CHCH), 108.8 (*pz*-NCHCH), 107.0 (*pz*-NCHCH), 63.4 (CH_2), 62.5 (CH_2). Due to the insensitivity of the ^{13}CO nucleus, this signal was not observed unless ^{13}C-enriched CO (99.5%) was used in the preparation of **15**. $^{13}C\{^1H\}$ NMR (100 MHz, acetone-d_6): δ 190.5 (d, ^1J(RhC) = 78.0 Hz, CO).

General Catalysis Procedures. All catalyzed reactions were performed under nitrogen in NMR tubes fitted with a Young's concentric Teflon valve. The samples were heated in an oil bath set at the desired temperature, and the reaction progress was monitored by ^{1}H NMR spectroscopy. Conversions were determined by comparison of the substrate and product integrals.[31−33] Reactions with CO containing catalysts were prepared from the corresponding COD complexes by degassing the reaction solution using two freeze–pump–thaw cycles and adding an atmosphere of CO to the head space. The solutions were shaken vigorously for several minutes prior to heating. For the bimetallic catalyst **15** half the stated amount of catalyst was used to maintain a constant Rh concentration across samples.

*Hydroamination of 5-Phenyl-4-pentyn-1-amine (**18**).* A stock solution of 5-phenyl-4-pentyn-1-amine (**18**) in 1,4-dioxane-d_8 (0.15 M) was prepared. The stock solution (0.6 mL) was then added to 4.5 μmol of catalyst (5 mol %) and heated at 100 °C for 12 h.

*Hydrocarboxylation of 4-Pentynoic Acid (**20**).* A stock solution of 4-pentynoic acid (**20**) in THF-d_8 (0.15 M) was prepared. The stock solution (0.6 mL) was then added to 4.5 μmol of catalyst (5 mol %) and heated at 80 °C for 24 h.

*Hydrosilylation of 1-Phenylpropyne (**22**) and Phenylacetylene (**24**).* A solution of the catalyst (2.5 μmol, 3 mol %) was prepared in acetone-d_6 (0.6 mL). To this was added the desired alkyne (83 μmol) and Et_3SiH (91 μmol) via microsyringe, and the solution was heated at 55 °C for 24 h.

■ ASSOCIATED CONTENT

Ⓢ Supporting Information

^{1}H and ^{13}C NMR spectra for all reported compounds, HRMS spectra for compounds **8**, **9**, **10**, and **15**, and CIF files for compounds **8**, **9**, **10**, **11**, **12**, and **15**. This material is available free of charge via the Internet at http://pubs.acs.org.

■ AUTHOR INFORMATION

Corresponding Author

*E-mail: b.messerle@unsw.edu.au.

Notes

The authors declare no competing financial interest.

■ ACKNOWLEDGMENTS

This research was supported under Australian Research Council's Discovery Projects funding scheme (project number

DP110101611). Financial support from the University of New South Wales is gratefully acknowledged. G. M. thanks the Australian government for an International Postgraduate Research Scholarship.

REFERENCES

(1) (a) Yamamoto, Y.; Radhakrishnan, U. *Chem. Soc. Rev.* **1999**, *28*, 199−207. (b) *Catalytic Heterofunctionlization*; Togni, A., Grützmacher, H., Eds.; Wiley-VCH: Weinheim, Germany, 2001. (c) Alonso, F.; Beletskaya, I. P.; Yus, M. *Chem. Rev.* **2004**, *104*, 3079−3159. (d) Nakamura, I.; Yamamoto, Y. *Chem. Rev.* **2004**, *104*, 2127−2198. (e) Müller, T. E.; Hultzsch, K. C.; Yus, M.; Foubelo, F.; Tada, M. *Chem. Rev.* **2008**, *108*, 3795−3892. (f) Lim, D. S. W.; Anderson, E. A. *Synthesis* **2012**, *44*, 983−1010. (g) Teles, J. H. In *Modern Gold Catalyzed Synthesis*; Hashmi, A. S. K., Toste, F. D., Eds.; Wiley-VCH: Weinheim, Germany, 2012; p 201.

(2) For lanthanide and alkaline earth catalysed reactions, see: (a) Weiss, C. J.; Marks, T. J. *Dalton Trans.* **2010**, *39*, 6576−6588. (b) Reznichenko, A. L.; Hultzsch, K. C. *Top. Organomet. Chem.* **2013**, *43*, 51−114.

(3) (a) Albrecht, M.; van Koten, G. *Angew. Chem., Int. Ed.* **2001**, *40*, 3750−3781. (b) Singleton, J. T. *Tetrahedron* **2003**, *59*, 1837−1857. (c) Van de Boom, M. E.; Milstein, D. *Chem. Rev.* **2003**, *103*, 1759−1792. (d) Dupont, J.; Consorti, C. S.; Spencer, J. *Chem. Rev.* **2005**, *105*, 2527−2571. (e) Selander, N.; Szabó, K. J. *Dalton Trans.* **2009**, 6267−6279. (f) Selander, N.; Szabó, K. J. *Chem. Rev.* **2011**, *111*, 2048−2076. (g) Szabó, K. J. *Top. Organomet. Chem.* **2013**, *40*, 203−241.

(4) For Ti, Zr, and Hf catalyzed reactions, see: (a) Cho, J.; Hollis, T. K.; Valente, E. J.; Trate, J. M. *J. Organomet. Chem.* **2011**, *696*, 373−377. (b) Helgert, T. R.; Hollis, T. K.; Valente, E. J. *Organometallics* **2012**, *31*, 3002−3009. (c) Luconi, L.; Rossin, A.; Motta, A.; Tuci, G.; Giambastiani, G. *Chem.—Eur. J.* **2013**, *19*, 4906−4921. (d) Luconi, L.; Klosin, J.; Smith, A. J.; Germain, S.; Schulz, E.; Hannedouche, J.; Giambastiani, G. *Dalton Trans.* **2013**, *42*, 16056−16065.

(5) For Ni, Pd and Pt catalyzed reactions, see: (a) Sui-Seng, C.; Castonguay, A.; Chen, Y. F.; Gareau, D.; Groux, L. F.; Zargarian, D. *Top. Catal.* **2006**, *37*, 81−90. (b) Castonguay, A.; Spasyuk, D. M.; Madern, N.; Beauchamp, A. L.; Zargarian, D. *Organometallics* **2009**, *28*, 2134−2141. (c) Adams, J. J.; Arulsamy, N.; Roddick, D. M. *Organometallics* **2009**, *28*, 1148−1157. (d) Lefevre, X.; Durieux, G.; Lesturgez, S.; Zargarian, D. *J. Mol. Catal. A* **2011**, *335*, 1−7. (e) Salah, A. B.; Offenstein, C.; Zargarian, D. *Organometallics* **2011**, *30*, 5352−5364. (f) Ogata, K.; Sasano, D.; Yokoi, T.; Isozaki, K.; Seike, H.; Takaya, H.; Nakamura, M. *Chem. Lett.* **2012**, *41*, 498−500.

(6) For Rh and Ir catalyzed reactions, see: (a) Andavan, G. T. S.; Bauer, E. B.; Letko, C. S.; Hollis, T. K.; Tham, F. S. *J. Organomet. Chem.* **2005**, *690*, 5938−5947. (b) Lai, R.-Y.; Surekha, K.; Hayashi, A.; Ozawa, F.; Liu, Y.-H.; Peng, S.-M.; Liu, S.-T. *Organometallics* **2007**, *26*, 1062−1068. (c) Bauer, E. B.; Andavan, G. T. S.; Hollis, T. K.; Rubio, R. J.; Cho, J.; Kuchenbeiser, G. R.; Helgert, T. R.; Letko, C. S.; Tham, F. S. *Org. Lett.* **2008**, *10*, 1175−1178.

(7) (a) Remenar, J. F.; Collum, D. B. *J. Am. Chem. Soc.* **1997**, *119*, 5573−5582. (b) Braunstein, P.; Naud, F. *Angew. Chem., Int. Ed.* **2001**, *40*, 680−699. (c) Weng, Z.; Teo, S.; Hor, T. S. A. *Acc. Chem. Res.* **2007**, *40*, 676−684.

(8) (a) Shi, P.-Y.; Liu, Y.-H.; Peng, S.-M.; Liu, S.-T. *Organometallics* **2002**, *21*, 3203−3207. (b) Bassetti, M.; Capone, A.; Salamone, M. *Organometallics* **2004**, *23*, 247−252. (c) Poverenov, E.; Gandelman, M.; Shimon, L. J. W.; Rozenberg, H.; Ben-David, Y.; Milstein, D. *Organometallics* **2005**, *24*, 1082−1090. (d) Niu, J.-L.; Hao, X.-Q.; Gong, J.-F.; Song, M.-P. *Dalton Trans.* **2011**, *40*, 5135−5150.

(9) (a) Gandelman, M.; Vigalok, A.; Shimon, L. J. W.; Milstein, D. *Organometallics* **1997**, *16*, 3981−3986. (b) Gandelman, M.; Shimon, L. J. W.; Milstein, D. *Chem.—Eur. J.* **2003**, *9*, 4295−4300.

(10) Zhang, J.; Leitus, G.; Ben-David, Y.; Milstein, D. *J. Am. Chem. Soc.* **2005**, *127*, 10840−10841.

(11) Lindner, R.; van den Bosch, B.; Lutz, M.; Reek, J. N. H.; van der Vlugt, J. I. *Organometallics* **2011**, *30*, 499−510.

(12) (a) Crudden, C. M.; Allen, D. P. *Coord. Chem. Rev.* **2004**, *248*, 2247−2273. (b) Hahn, F. E.; Jahnke, M. C. *Angew. Chem., Int. Ed.* **2008**, *47*, 3122−3172.

(13) (a) Diez-González, S.; Marion, N.; Nolan, S. P. *Chem. Rev.* **2009**, *109*, 3612−3676.

(14) (a) Chen, J. C. C.; Lin, I. J. B. *Organometallics* **2000**, *19*, 5113−5121. (b) Catalano, V. J.; Malwitz, M. A.; Etogo, A. O. *Inorg. Chem.* **2004**, *43*, 5714−5724. (c) Lee, H. M.; Zeng, J. Y.; Hu, C.-H.; Lee, M.-T. *Inorg. Chem.* **2004**, *43*, 6822−6829. (d) Zeng, J. Y.; Hsieh, M.-H.; Lee, H. M. *J. Organomet. Chem.* **2005**, *690*, 5662−5671. (e) Schneider, N.; César, V.; Bellemin-Laponnaz, S.; Gade, L. H. *Organometallics* **2005**, *24*, 4886−4888. (f) Gu, S.; Xu, H.; Zhang, N.; Chen, W. *Chem.—Asian J.* **2010**, *5*, 1677−1686. (g) Fliedel, C.; Sabbatini, A.; Braunstein, P. *Dalton Trans.* **2010**, *39*, 8820−8828. (h) Newman, P. D.; Cavell, K. J.; Hallett, A. J.; Kariuki, B. M. *Dalton Trans.* **2011**, *40*, 8807−8813. (i) Al Thagfi, J.; Lavoie, G. G. *Organometallics* **2012**, *31*, 2463−2469. (j) Chen, C.; Qiu, H.; Chen, W. *J. Organomet. Chem.* **2012**, *696*, 4166−4172.

(15) (a) Esteruelas, M. A.; Oro, L. A. *J. Organomet. Chem.* **1989**, *366*, 245−255. (b) Padilla-Martínez, I. I.; Poveda, M. L.; Carmona, E. *Organometallics* **2002**, *21*, 93−104. (c) Montag, M.; Efremenko, I.; Cohen, R.; Shimon, L. J. W.; Leitus, G.; Diskin-Posner, Y.; Ben-David, Y.; Salem, H.; Martin, J. M. L.; Milstein, D. *Chem.—Eur. J.* **2010**, *16*, 328−353.

(16) (a) Mann, K. R.; Gordon, J. G., II; Gray, H. B. *J. Am. Chem. Soc.* **1975**, *97*, 3553−3555. (b) Mann, K. R.; Lewis, N. S.; Williams, R. M.; Gray, H. B.; Gordon, J. G., II. *Inorg. Chem.* **1978**, *17*, 828−834.

(17) Messerle, B. A.; Page, M. J.; Turner, P. *Dalton Trans.* **2006**, 3927−3933.

(18) Burling, S.; Field, L. D.; Messerle, B. A.; Rumble, S. L. *Organometallics* **2007**, *26*, 4335−4343.

(19) (a) Chan, D. M. T.; Marder, T. B.; Milstein, D.; Taylor, N. J. *J. Am. Chem. Soc.* **1987**, *109*, 6385−6388. (b) Elgafi, S.; Field, L. D.; Messerle, B. A. *J. Organomet. Chem.* **2000**, *607*, 97−104.

(20) Mas-Marza, E.; Sanau, M.; Peris, E. *Inorg. Chem.* **2005**, *44*, 9961−9967.

(21) Poyatos, M.; Maisse-Francois, A.; Bellemin-Laponnaz, S.; Gade, L. H. *Organometallics* **2006**, *25*, 2634−2641.

(22) Jiménez, M. V.; Pérez-Torrente, J. J.; Bartolomé, M. I.; Gierz, V.; Lahoz, F. J.; Oro, L. A. *Organometallics* **2008**, *27*, 224−234.

(23) Busetto, L.; Cassani, M. C.; Femoni, C.; Mancinelli, M.; Mazzanti, A.; Mazzoni, R.; Solinas, G. *Organometallics* **2011**, *30*, 5258−5272.

(24) Watson, A. A.; House, D. A.; Steel, P. J. *Aust. J. Chem.* **1995**, *48*, 1549−1572.

(25) Burling, S.; Field, L. D.; Messerle, B. A.; Vuong, K. Q.; Turner, P. *Dalton Trans.* **2003**, 4181−4191.

(26) Giordano, G. C.; Crabtree, R. H. *Inorg. Synth.* **1990**, *28*, 88−90.

(27) Herde, J. L.; Lambert, J. C.; Senoff, C. V.; Cushing, M. A. *Inorg. Synth.* **1974**, *15*, 18−20.

(28) Fukuda, Y.; Martsubara, S.; Utimoto, K. *J. Org. Chem.* **1991**, *56*, 5812−5816.

(29) Sheldrick, G. M. *Acta Crystallogr.* **2008**, *A64*, 112−122.

(30) Julia, S.; Martinez-Martorell, C.; Elguero, J. *Heterocycles* **1986**, *24*, 2233−2237.

(31) For hydroamination of 5-phenyl-4-pentyn-1-amine (**22**), see: Li, Y.; Marks, T. J. *J. Am. Chem. Soc.* **1996**, *118*, 9295−9306.

(32) For hydrocarboxylation of 4-pentynoic acid (**24**), see: Amos, R. A.; Katzenellenbogen, J. A. *J. Org. Chem.* **1978**, *43*, 560−564.

(33) For hydrosilylation of 1-phenylpropyne (**26**) and phenylacetylene (**28**), see: Field, L. D.; Ward, A. J. *J. Organomet. Chem.* **2003**, *681*, 91−97.